Patterns of polymorphism, selection and linkage disequilibrium in the subgenomes of the allopolyploid *Arabidopsis kamchatica*

Timothy Paape[1*], Roman V. Briskine[1,2], Heidi E.L Lischer[1,3], Gwyneth Halstead-Nussloch[1], Rie Shimizu-Inatsugi[1], Masaomi Hatekayama[1,2,3], Kenta Tanaka[4], Tomoaki Nishiyama[5], Renat Sabirov[6], Jun Sese[7], Kentaro K. Shimizu[1,8*]

[1] Department of Evolutionary Biology and Environmental Studies and Department of Plant and Microbial Biology, University of Zurich, Winterthurerstrasse 190, CH-8057 Zurich, Switzerland

[2] Functional Genomics Center Zurich, Winterthurerstrasse 190, CH-8057 Zurich, Switzerland

[3] Swiss Institute of Bioinformatics (SIB), Lausanne, Switzerland

[4] Sugadaira Montane Research Center, University of Tsukuba, Ueda, Nagano, Japan

[5]Advanced Science Research Center, Kanazawa University, 13-1 Takara-machi, Kanazawa, 920-0934, Japan

[6] Institute of Marine Geology and Geophysics, Far East Branch, Russian Academy of Sciences, Yuzhno-Sakhalinsk, Russia

[7] Artificial Intelligence Research Center, National Institute of Advanced Industrial Science and Technology (AIST), Tokyo, Japan

[8] Kihara Institute for Biological Research, Yokohama City University, 641-12 Maioka, 244-0813 Totsuka-ward, Yokohama, Japan.

*authors for correspondence

Abstract

Although genome duplication is widespread in wild and crop plants, little is known about genome-wide selection due to the complexity of polyploid genomes. In allopolyploid species, the patterns of purifying selection and adaptive substitutions would be affected by masking owing to duplicated genes or 'homeologs' as well as by effective population size. We resequenced 25 distribution-wide accessions of the allotetraploid *Arabidopsis kamchatica*, which has a relatively small genome size (450 Mb) derived from the diploid species *A. halleri* and *A. lyrata*. The level of nucleotide polymorphism and linkage disequilibrium decay were comparable to *A. thaliana*, indicating the feasibility of association studies. A reduction in purifying selection compared with parental species was observed. Interestingly, the proportion of adaptive substitutions (α) was significantly positive in contrast to the majority of plant species. A recurrent pattern observed in both frequency and divergence-based neutrality tests is that the genome-wide distributions of both subgenomes were similar, but the correlation between homeologous pairs was low. This may increase the opportunity of different evolutionary trajectories such as in the *HMA4* gene involved in heavy metal hyperaccumulation.

Introduction

Genome duplication is a widespread evolutionary force in plants. As many as 35% of vascular plants are recent polyploid species[1] and increased ploidy is particularly common in crops[2]. The abundance of polyploid species in plants motivated speculation and theoretical analysis on the advantages and disadvantages of genome duplication[3,4]. However, compared with diploid species, much less is known about the genome-wide patterns of polymorphism and selection due to the complexity of polyploid genomes[5]. Major difficulties in genome scale analyses result from the large genome sizes of polyploids and the high similarity between the duplicated chromosomes. However, recent advances in next-generation sequencing and bioinformatic tools[6,7] are enabling genome-wide data to study polymorphisms and transcriptomics patterns for entire subgenomes in newly emerging model polyploids[8–11].

Genome-wide strengths of positive and purifying selection can be quantified using several complementary approaches. Frequency-based tests using site-frequency spectra (SFS) such as Tajima's *D* and Fay and Wu's *H* statistics can detect rare or common polymorphisms that are due to purifying or positive selection. Divergence-based tests compare interspecific divergence (from an outgroup) to intraspecific polymorphism to identify positive selection on amino-acid substitutions[12]. These tests include several derivatives of the McDonald-Kreitman test[13] or "MK-tests", such as the direction of selection (DoS) neutrality index[14], and methods to estimate the distribution of fitness effects (DFE) and proportion of adaptive substitutions (α)[13] in genome-wide data. Theoretical and empirical studies in plant species using these methods[15,16] showed that the strengths of selection are affected by species-specific characteristics such as the effective population size (N_e), mating system, and genome duplication, which are mutually interacting. In particular, species with low N_e typically have the highest proportions of neutral mutations[15,17], while species with large N_e have higher proportions of non-synonymous substitutions under purifying selection and adaptive evolution[8,19,20].

Allopolyploidization should have a profound effect on the patterns of polymorphism and selection. First, the redundancy of duplicated gene copies of similar function from different parents ("homeologs") may affect the strength of selection. At the early stages, genome duplication may increase evolutionary rates of duplicated genes[21,22] and may facilitate the evolution of new adaptive function because the original function can be retained in other copies (so-called neofunctionalization model)[23,24]. In contrast, the additional copy may mask the effect of adaptive and deleterious mutations[4,16]. Second, polyploidization must involve a reduction in

N_e due to a bottleneck during speciation. In addition, polyploid speciation is typically associated with the transition from outcrossing to self-fertilization, which reduces N_e several times less than parental species (at least half)[25]. While studies of selection in polyploids are very limited, a recent empirical study in the allotetraploid *Capsella bursa-pastoris* showed a decrease in the efficacy of purifying selection in one of the subgenomes but an increase in another subgenome[8]. Further empirical studies are necessary to compare the consequences of genome duplication in polyploid species.

The genus *Arabidopsis* has both auto- and allopolyploid species in addition to the more well-studied diploid relatives[26]. *Arabidopsis kamchatica*[27] is a recent allopolyploid (estimated 20,000-250,000 years ago)[28] derived from the two diploid species *A. halleri* (particularly subsp. *gemmifera* distributed in East Asia), and *A. lyrata* (particularly subsp. *petraea* from Far East Russia)[29–31]. The two diploid parents are predominantly self-incompatible (SI) while a transition to selfing accompanied allopolyploid formation[28]. The genome size (about 450 Mb) is relatively small among polyploid species[32,33] which is an advantage for resequencing. The species distribution of *A. kamchatica* is very broad, ranging from Taiwan, Japan, Far East Russia, Alaska and Pacific Northwest, USA. The high variation in latitude and altitude compared with the parental species[34,35] suggests that merging the diploid transcriptional networks and parental adaptations provided the allopolyploid with plasticity to inhabit diverse environments[10].

To understand the ecological distributions of polyploids, genetically tractable traits are essential. Heavy metal tolerance and hyperaccumulation likely influenced ecological divergence and speciation between the parental species of *A. kamchatica* (*A. halleri* and *A. lyrata*) due to adaptive mutations in metal transporter genes such as *HEAVY METAL ATPASE4* (*HMA4*)[36,37]. The *HMA4* locus has been shown to be the primary transporter of cadmium and zinc from roots to shoots in *A. halleri* due to a tandem triplication and enhanced *cis*-regulation, while only a single copy of *HMA4* exists in the non-hyperaccumulators *A. lyrata* and *A. thaliana*. *A. kamchatica* inherited hyperaccumulation from the diploid parent *A. halleri*, although attenuated expression of *halleri*-derived *HMA4* and putatively inhibiting *lyrata*-derived factors reduced the trait to about half of *A. halleri*[10]. Estimates of genetic diversity surrounding the *HMA4* region in *A. halleri* suggests a hard selective sweep[38] which may have predated the formation *A. kamchatica*[10].

Here, we used *de novo* assemblies of the closest diploid relatives of *A. kamchatica* to sort Illumina reads to their respective subgenomes using a distribution-wide collection of 25 natural allopolyploid accessions. We used population genomics to ask: a) what is the level of

genome-wide diversity compared with diploid outcrossing and selfing *Arabidopsis* species? b) are there differences in polymorphism, allele frequencies, linkage disequilibrium (LD), and selection between subgenomes? c) do pairs of homeologs tend to show similar patterns in diversity and neutrality? d) does the *HMA4* locus show significant differences in genetic diversity between homeologs and how does diversity surrounding this locus compare with the genome-wide average? e) what proportions of the subgenomes show neutral, deleterious, or adaptive mutations and how do they differ from the diploid parents? and f) are there high frequencies of loss of function mutations in either subgenome? Together, these plant accessions and polymorphism data will serve as a core diversity panel for further studies of genotype-phenotype associations and the genetic architecture of complex traits using larger collections of globally collected samples.

Results

Reference Genome Assembly and Allopolyploid Resequencing

To sort Illumina reads of *A. kamchatica* to their parentally-derived subgenomes, we generated long mate-pair *de novo* assemblies of *A. lyrata* subsp. *petraea* (also called *A. petraea* subsp. *umbrosa*) in addition to East Asian *A. halleri* subsp. *gemmifera* which we previously reported[39]. Assembly statistics indicated that the *A. lyrata* and *A. halleri* reference genomes have scaffold N50 of 1.2 Mb and 0.7 Mb, comprising 1,675 and 2,239 scaffolds respectively (Table 1, Supplementary Table 1 and 2 for gene annotation statistics), providing opportunities to compare diversity over very large syntenic regions in the allopolyploid subgenomes.

We sorted reads of 25 individuals from a distribution-wide collection (Supplementary Table 3) of *A. kamchatica* to their parental origins by first aligning each read to both parental genomes then classified the reads as '*origin*' reads (*halleri*-derived = H-origin, *lyrata*-derived = L-origin) using algorithms that quantify mismatches to either parent[32]. Our accessions had on average 12.5X coverage for the H-origin-subgenome (range 5.2X - 20.7X) and on average 10.7X coverage for the L-origin-subgenome (range 4.3X - 17.7X). Homeolog specific PCR and Sanger sequencing was used to validate SNPs and read sorting for twelve genes and showed that reads were accurately assigned to their respective subgenomes (Supplementary Material). In addition, pyrosequencing was used in two previous studies to detect ratios of parentally derived SNPs to validate homeolog specific expression (RNA-seq) in ten other genes[10,32] where the same read sorting pipeline was used. After filtering for SNP quality and coverage, our resequencing dataset

resulted in 1,674,191 H-origin and 1,930,341 L-origin SNPs. Using the parental genome assemblies for *A. kamchatica* SNP calling, we identified ca. 23,500 homeologous coding sequences using reciprocal best BLAST hits (Supplementary Table 2), of which ca. 21,500 show orthology to *A. thaliana*, representing 72% and 67% of our annotated genes respectively.

Genome-wide Nucleotide Diversity in *A. kamchatica*

We examined the patterns of nucleotide diversity for ca. 21,000 coding sequences of both *halleri* and *lyrata*-derived homeologs in *A. kamchatica* that could be aligned to *A. thaliana* orthologs as the outgroup. We found that both subgenomes showed similar mean values of nucleotide diversity (π) (π_{coding} = 0.0014 bp^{-1} for *halleri*-subgenome and π_{coding} = 0.0015 bp^{-1} for *lyrata*-subgenome, and π_{coding} = 0.0015 bp^{-1} when combined) although the *lyrata*-derived homeologs showed slightly broader ranges in π (Table 2, Fig. 1A). Nucleotide diversity at synonymous sites (π_{syn}) was also similar for the two subgenomes with a slightly higher value for the *lyrata*-subgenome (π_{syn} = 0.0049) than in the *halleri*-subgenome (π_{syn} = 0.0044). The nucleotide diversity in *A. kamchatica* is about six times lower than European *A. halleri* and *A. lyrata* (π_{syn} = 0.029 for *A. halleri* and 0.028 for *A. lyrata* estimated using resequencing data from[30]) and is more similar to that of *A. thaliana* (π_{syn} = 0.0059 - 0.007)[17,30,40]. Sliding window analysis including non-coding regions also showed comparable values (Supplementary Table 4).

We calculated the effective population size, N_e, using our empirical estimates of π for *A. kamchatica* and both diploid species and two different mutation rates[41,42]. The estimated values for *A. kamchatica* were: N_e = 77,000 and 54,000 using the two mutation rates respectively. The values for *A. kamchatica* were several times lower than *A. halleri*: N_e = 467,000 and 364,000 and *A. lyrata*: N_e = 483,000 and 345,000 (Supplementary Table 5). We interpret these estimates of N_e with caution as the mutation rates for these species have not been estimated directly and the diversity estimates used in the calculation can themselves be affected by demography. The estimates are nevertheless useful as general comparisons between species to identify large differences in magnitude[17,19].

Higher proportions of non-synonymous mutations were found to be at low frequency compared with synonymous mutations and no significant differences in the relative proportions were found between subgenomes (Fig. 1B). This suggests purifying selection on a large proportion of amino-acid changing substitutions in both subgenomes. Frequency-based test statistics clearly show significant departures from neutrality for both subgenomes (Fig. 1C). The

mean values of Tajima's D were negative for both subgenomes (Table 2, Fig. 1C) owing to high proportions of rare variants.

The distributions and means of Tajima's D in *A. kamchatica* (Table 2) are similar to early genome-wide data from *A. thaliana* (mean Tajima's $D_{A.thaliana}$ = -0.8)[43], although more recent estimates using over 300 genomes show a higher mean but not higher median in *A. thaliana* (mean $D_{A.thaliana}$ = 0.006, median $D_{A.thaliana}$ = -0.33)[30], which likely reflects more intermediate-frequency polymorphisms in the large species wide sample. The same study[30] reported an excess of rare variants in the diploid relatives of *A. kamchatica* (mean $D_{A.lyrata}$ to be -0.99 in *A. lyrata* and $D_{A.halleri}$ = -0.23 in *A. halleri*).

We found the means of the distributions for most summary statistics to be very similar between the two subgenomes, but when pairs of all homeologs were compared correlations were generally low for diversity and neutrality estimators (Table 2). The correlations of π_{syn} and $\theta_{w\,syn}$ were both nearly zero (Table 2). Similarly, the distributions and means of Tajima's D overlap for both subgenomes but the correlation for Tajima's D between pairs of homeologs is very low (R^2 = 0.03). The Fay and Wu's H statistic, which detects departures from neutrality due to intermediate and high frequency variants, also shows a very low correlation between homeologs (Table 2). Higher correlations were observed for non-synonymous or total sites, but this can be explained by the constraints on non-synonymous changes. In summary, the low correlations are consistent with different evolutionary trajectories of individual homeologous pairs.

Mean Rate of LD Decay in Both Subgenomes is Similar But Not Equal

Long scaffold assemblies allowed us to estimate genome-wide LD for each subgenome to evaluate the feasibility of association mapping in *A. kamchatica*. We found that mean LD decay was between 5-10 kb for both subgenomes (Fig. 1D), which is similar to the self-fertilizing species *A. thaliana* and *M. truncatula* which show LD decay within 2-10 kb ranges[44,45]. The mean LD for the *lyrata*-subgenome decayed slightly faster and remained at r^2 = 0.47 over the scale of > 100 kb genomic regions while mean LD for the *halleri*-subgenome leveled off at r^2 = 0.34 > 100 kb. The 50% and 90% confidence intervals around the mean LD decay also revealed much greater variance in the *lyrata*-subgenome (Supplementary Fig. 1).

Population structure assignments and phylogenetic clustering may provide some explanation for subgenome differences in LD. The 25 accessions cluster geographically with one

main clade/group comprising the northern accessions (Russia, Sakhalin, and Alaska) and the other main group containing Japanese accessions (Supplementary Fig. 2,3). The branch lengths within these groups for the *lyrata*-subgenome are shorter than for the *halleri*-subgenome, particularly in the Japanese clade, indicating greater relatedness. These clusterings are also consistent with previous haplotype analysis using low density nuclear and chloroplast markers[29].

Diversity of the *HMA4* Locus and the Genomic Background

We analyzed genetic diversity on the scaffolds containing the *HMA4* locus to compare whether it differs from the genomic background and the surrounding regions flanking the *HMA4* coding sequences. We centered the main genomic region containing the *HMA4* coding sequences which we call "HMA4-M" (containing 17 coding sequences). This region spans 304 kb on *A. halleri* (scaffold_116) and spans 155 kb on *A. lyrata* (scaffold_52). While the differences in length of HMA4-M between the parental genomes can be attributed to the triplicated *HMA4* genes in *A. halleri*, the genes surrounding *HMA4* in both *A. halleri* and *A. lyrata* are syntenic (Fig. 2A). To compare HMA4-M to surrounding regions, we used the upstream adjacent region (left-side) "HMA4-L" (containing 13 coding sequences) which is 125 kb for the *A. halleri* region and 183 kb in *A. lyrata*, and the downstream adjacent region (right-side) "HMA4-R" (containing 13 CDS sequences), which is 105 kb in the *A. halleri* region and ca. 50 kb for *A. lyrata*.

The distribution of π in the HMA4-M region for H-origin genes showed low diversity (π_{mean} = 0.0007) but it is not significantly lower than the background genes (Fig. 2B and 2C). However, the two adjacent regions (HMA4-L and HMA4-R) compared to the HMA4-M (containing the *HMA4* coding sequences) region have significantly greater diversity (Fig. 2B and 2C). Furthermore, we found significantly lower Tajima's D, Fu & Li's D* and Fu & Li's F* statistics in the HMA4-M region compared with both adjacent regions (Fig. 2E), suggesting greater selection on the HMA4-M region. The significantly lower diversity and neutrality statistics in HMA4-M compared with the adjacent regions likely defines the window of the sweep region previously reported for *A. halleri* [38].

Unlike the *halleri* HMA4-M region, the diversity of the *lyrata* HMA4-M region is significantly greater than the genomic background (p-value = 0.0028), but not different from the two adjacent regions (Fig. 2D). Moreover, the *lyrata*-HMA4-M region shows no significant differences from the adjacent HMA4-L or HMA4-R regions for Tajima's D, Fu & Li's D* and Fu & Li's F* (not shown). The elevated diversity of the *lyrata*-origin *HMA4* locus compared with the

genomic background is consistent with relaxed selective constraint on the *lyrata*-origin *HMA4* locus.

We also estimated diversity of all annotated heavy metal transporters, metal ion transporters, and metal homeostasis genes for comparison with the genome-wide average (HM genes, N=118 genes). We expected these genes to have low overall diversity in both genomes due to selective constraint as many of these ion transporters are expected to have roles in basic metal homeostasis[46]. As a contrast, we compared NBS-LRR genes (N=39 genes) which have putative roles in plant defense and have high diversity in plants[47,48] and are expected to have equally high diversity in both subgenomes. The HMA4-L and HMA4-R regions in both subgenomes have more similar levels of diversity to NBS-LRR's than to the genomic background or HM genes (Fig. 2C and 2D).

The Majority of Homeologous Proteins Showed Signatures of Purifying Selection

Next we employed divergence-based tests to estimate the strength of purifying and positive selection on amino-acid changing substitutions. We calculated the divergence of each homeolog from the outgroup *A. thaliana* to estimate the relative proportions of diverged non-synonymous (D_n) and synonymous (D_s) sites to polymorphic non-synonymous (P_n) and synonymous (P_s) sites. For each gene, The counts of D_n, D_s, P_n, and P_s for the coding regions of both subgenomes were used to estimate the direction of selection (DoS)[14], a neutrality index that varies from -1.0 to 1.0, where zero indicates neutrality and negative and positive values indicate purifying and positive selection, respectively. Both subgenomes had similar distributions in DoS with means of -0.2 (Fig. 3A) suggesting that 68-71% of proteins derived from both subgenomes are under purifying selection (when DoS is < -0.01). Like the previous summary statistics, the correlation in DoS between *halleri* and *lyrata* homologs is positive but fairly low ($R^2 = 0.17$).

MK-tests were conducted to detect homeologs showing purifying selection or adaptive evolution on amino-acid changing mutations. Among the significant MK-test genes, a total of 3018 H-origin and 3804 L-origin homeologs showed DoS < 0 ($D_n/D_s < P_n/P_s$). This is consistent with purifying selection rather than positive selection for these genes. While the homeologs with significant MK-test comprise a substantial portion in our dataset, only 19% of them include both homeologs (i.e., there is significance for one homeolog but not the other for 81% of significant homeologous pairs, Fig. 3B). For example, the H-origin homeolog of the resistance

gene *RPM1* (orthologous to *A. thaliana* gene: AT3G07040) was significant for the MK-test (DoS < 0) but the L-origin copy was not.

For genes showing positive selection (or adaptive evolution) using MK-tests, 146 *halleri*-origin and 212 *lyrata*-origin genes were significant when DoS > 0.01 (Fig. 3C, D). For these genes, when the *halleri*-derived homeologs shows a positive DoS, the *lyrata*-derived homeolog shows a more neutral or negative distribution in DoS and vice versa. Among these is the H-origin *HMA4* gene. These results, in addition to the low correlation in DoS between homeologous pairs and small overlap among all significant MK-test genes (Fig. 3B), indicates that a substantial proportion of homeologs have been shaped by different strengths of selection. These results are also in agreement with low correlations in Tajima's D and Fay and Wu's H despite for pairs of homeologs (Table 1), providing additional support that redundant genes exhibit significant differences due to stronger positive or purifying selection on only one of the two copies.

The Distribution of Fitness Effects (DFE)

The tests above indicated that large numbers of homeologs show patterns consistent with purifying selection on amino-acid changing mutations (see Fig. 3). We quantified the genome-wide proportions of deleterious and effectively neutral mutations using the distribution of fitness effects (DFE) method[13] in the two *A. kamchatica* subgenomes and both diploid relatives. In this method, the DFE is estimated from the site frequency spectra of non-synonymous and synonymous polymorphisms while accounting for effects of demographic changes. Effectively neutral mutations are represented by $0 < N_e s < 1$, mildly deleterious by $1 < N_e s < 10$, deleterious by $10 < N_e s < 100$ and strongly deleterious by $N_e s > 100$ (where N_e is the effective population size and s is the selection coefficient). The DFE estimates of the two *A. kamchatica* subgenomes show similar distributions with about 70% of mutations in the deleterious to strongly deleterious categories ($N_e s > 10$) and about 20% effectively neutral ($0 < N_e s < 1$) (Fig. 4A). The DFE of *A. halleri* and *A. lyrata* showed lower proportions of neutral mutations (16% of mutations $0 < N_e s < 1$ in diploids, and 19% mutations $0 < N_e s < 1$ in both subgenomes) and greater proportions of deleterious mutations ($N_e s > 100$) than either of the corresponding allopolyploid subgenomes. While the differences are significant, the magnitude of the differences is not remarkable.

To examine whether subsets of either subgenome experience a reduction in purifying selection, we classified homeologs according to gene expression level, which is one of the best predictors of evolutionary rates (dN/dS) in most organisms[49]. Expression level is negatively

correlated with dN/dS due to strong constraint on amino acid substitutions (dN)[22] for highly expressed genes, but this has not been shown in recent polyploid species. As a test of selective constraint on highly expressed genes, we found dN/dS was negatively correlated with expression for both homeologs (Fig. 4B). We would therefore expect genes that are highly expressed to show the strongest purifying selection, and low expressed genes to show relaxed constraint. We estimated the DFE again to quantify purifying selection and relaxed constraint using the distribution of expression levels in leaf and root tissues of *A. kamchatica* to categorize homeologs as high (genes in upper 10% RPKM) or low expression (lower 10% of RPKM). The majority (62%) of the highly expressed genes include both homeologs (Fig. 4C). The DFE patterns indicated that low expressed genes have the highest proportion of neutral mutations (relaxed constraint) and the lowest proportion of deleterious mutations compared with the genome-wide data, while highly expressed genes showed the opposite pattern (Fig. 4D). These results indicate that the DFE method can detect relaxed constraint and strong purifying selection as predicted when gene expression levels are accounted for.

The Proportion of Adaptive Substitutions in Diploids and Allopolyploid Subgenomes

The proportion of adaptive substitutions (α) was estimated as the excess of between-species divergence relative to polymorphism as expected from the estimated DFE[13] to account for slightly deleterious mutations. In contrast to the majority of the previously studied plant species including *A. thaliana*, we found significantly positive values of α for the two diploid species and both allopolyploid subgenomes. The diploid species *A. halleri* and *A. lyrata* showed the highest α values (0.25 and 0.27 respectively) (Fig. 4E). We subsampled 18 *A. kamchatica* accessions to be statistically comparable to the available *A. halleri* and *A. lyrata* samples (Supplementary Table 6). The α estimates for the H- and L-origin subgenomes of *A. kamchatica* were lower than those of the corresponding diploid species but significantly greater than zero (0.12 and 0.09, respectively) (Fig. 4E). The difference in α between subgenomes was significant but subtle (3% difference using the samples above, 6% difference when all 25 *A. kamchatica* accessions were used; Supplementary Fig. 4).

High Impact Mutations are at Low Frequency in Subgenomes

We identified genes having high impact mutations that are likely to be deleterious due to their putative effects on amino acid sequences and gene expression into the following mutation

categories: frameshifts, loss of start codon, premature stop codons (stop gained), and loss of stop codons (stop loss). For any gene, we counted every one of the mutation types regardless of the number. While it is not possible to determine the order of disruptive mutations, multiple frameshifts of premature stop codons in a gene would be expected to result in a loss of function.

Frameshifts and stop-gained categories comprised the majority of mutation types for both subgenomes (Supplementary Table 7). Frequencies of each mutation type indicated that most mutation types in any gene are found in only a single genotype in either subgenome (Fig. 5). Despite a higher number of mutations in the *lyrata*-homeologs, there were slightly greater proportions at low frequencies in the *halleri*-homeologs. Out the total 4219 *halleri*-origin and 4952 *lyrata*-origin disrupted genes, only 511 genes (2.5%) showed large effect mutations in both homeologs in the same accession suggesting that large effect mutations in both homeologs were deleterious. The distribution of genes with high impact mutations in both homeologs shows that most accessions have < 50 genes (orthologous to *A. thaliana*) that are disrupted with putatively similar functions (Supplementary Fig. 5).

We conducted gene ontology (GO) analysis to determine whether there was enrichment for GO terms using the two most common high-impact mutation types, i.e., frameshift mutations and stop codons. For both subgenomes, hydrolase activity (GO:0016787) was the most significant GO term for molecular function, followed by several GO categories for nucleotide binding (Supplementary Table 8). Programmed cell death (GO:0012501) and apoptosis (GO:0006915) were significant in the *halleri*-origin genes only. No significant gene ontologies were found with ≥ 20 query genes for the list of genes that had high impact mutations in both homeologs in a single accession.

Discussion

Similar Genome-wide Distributions in Both Subgenomes but Low Correlations Between Homeologous Pairs

A recurrent pattern we observed on patterns of diversity and signatures of selection was that the genome-wide distributions were similar between subgenomes, but the correlations between the pairs of homeologs were low. We found this pattern in the polymorphism levels such as π_{syn} and $\theta_{w\,syn}$, in frequency-based tests of neutrality (Tajima's D, Fay & Wu's H), and in divergence-based tests (DoS). The similar genome-wide distributions are consistent with the fact that the subgenomes shared the same history since the allopolyploidization event. The low correlation

389 suggests that at the gene level, genetic diversity of a large number of homeologs may have been
390 shaped by different levels of positive and purifying selection, as well as relaxed constraint. This
391 supports that homeologs may evolve as independent loci, which may not be surprising because
392 *A. kamchatica* shows disomic inheritance prohibiting recombination between homeologs[28].
393 These results also suggest that the difference between homeologs could contribute to the broad
394 environmental response of polyploids, which may be realized by combining different
395 adaptations of two parental species[10] such as in the *HMA4* gene.
396
397 ## Nucleotide Diversity and Linkage Disequilibrium is Similar to *A. thaliana* Suggesting the
398 ## Feasibility of Genome-wide Association Studies of *A. kamchatica*
399 We found that the level of nucleotide diversity of *A. kamchatica* is moderate and similar to that
400 of the diploid self-compatible *A. thaliana,* and 6 times lower than the diploid outcrossing species
401 *A. halleri* and *A. lyrata*. It follows that the N_e of *A. kamchatica* is 6 times lower than the two
402 diploid species. The ancestor of the genus *Arabidopsis* must have been a self-incompatible
403 diploid species like present-day *A. lyrata* and *A. halleri*[25], indicating that similar reductions in
404 genetic diversity occurred in the lineages of *A. kamchatica* and *A. thaliana*.
405 The extent of LD decay in *A. kamchatica* is also comparable to *A. thaliana*[45] and appears
406 adequate for characterizing the genetic architecture of complex traits within relatively narrow
407 genomic windows using genome-wide association studies (GWAS). The selfing mating system,
408 levels of genetic diversity, LD, and a recently established transgenic technique[50] suggests that *A.*
409 *kamchatica* would be a suitable model for functional genomics of adaptive mutations in a
410 polyploid species.
411
412 ## The *HMA4* Locus Exhibits Significant Subgenome Differences in Genetic Diversity
413 The most important locus for zinc hyperaccumulation, *HMA4*[37], involved two types of gene
414 duplication in *A. kamchatica*: a tandem triplication in diploid *A. halleri*, followed by a whole
415 genome duplication event, which contributed an additional *HMA4* copy from the *A. lyrata*
416 parent. Despite multiple hybrid origins of *A. kamchatica*, the tandem triplication (three *halleri*-
417 derived *HMA4* copies) is fixed in the allopolyploid[10] suggesting it was present in all founding *A.*
418 *halleri* parents. The high expression of H-origin *HMA4* in *A. kamchatica* explains high levels of
419 zinc accumulation. Expression of the L-origin *HMA4* copy is very low compared with the *halleri*

HMA4 gene(s) so it is unlikely that the copy from *A. lyrata* contributes anything significant to hyperaccumulation in *A. kamchatica.*

Long scaffolds containing the *HMA4* copies and surrounding genes allowed us to compare homeologs across large genomic distances. The genetic diversity surrounding the *halleri*-derived *HMA4* gene that spans ca. 300 kb (HMA4-M) is significantly lower that the syntenic *lyrata*-derived region (ca. 100 kb) suggesting different evolutionary pressures or trajectories of functional duplicates. The higher diversity of the *lyrata* HMA4-M region is consistent with a pattern of relaxed constraint, while a selective sweep and genetic hitchhiking characterizes the *halleri*-derived HMA4-M region. Because we can infer that the triplication was ancestral and the reduced diversity at this locus and hitchhiking surrounding the *HMA4* genes was most likely the result of strong selection in the *A. halleri* parent[38], diversity was probably greatly reduced prior to the polyploidization events.

Purifying Selection in Polyploid Species

Theoretical studies suggested that higher proportions of neutral mutations (i.e., greater relaxed constraint) can result from whole genome duplication due to the reduction of N_e or due to masking of deleterious mutations by functionally redundant gene copies[15,16]. This would be evident by greater proportions of effectively neutral mutations ($0 < N_e s < 1$) in the polyploid subgenomes compared with the diploid parents[8]. Similarly, greater proportions of deleterious mutations ($N_e s > 10$) in the diploid species would be expected compared to their derived polyploid subgenomes. We did detect significant differences between diploid parental species and the corresponding subgenomes of *A. kamchatica* in the proportions of mutations in the neutral (< 5% differences) and deleterious (5-7% differences) categories, although the differences were not drastic (Fig. 4A).

Using a similar approach, the change in purifying selection was studied by comparing the allopolyploid species *C. bursa-pastoris* with its diploid parents, *C. grandiflora* (outcrosser with high N_e) and *C. orientalis* (selfing with low N_e)[8]. First, for the subgenome derived from the outcrossing parent *C. grandiflora,* the proportion of neutral mutations doubled from ~17% to ~35% neutral mutations. This demonstrated that the subgenome derived from an outcrossing parent with a large N_e shows a high proportion of neutral mutations due to relaxed constraint. Second, the opposite pattern was observed in the subgenome derived from the selfing parent (decreased from ~40% to 35% neutral mutations). The DFE patterns in *C. bursa-pastoris* and *C.*

orientalis conforms to the trend in plants which shows species with low N_e usually have greater proportions of neutral mutations[15] consistent with greater strengths of purifying selection with higher N_e. However, despite relatively high N_e and outcrossing mating systems in *A. halleri* and *A. lyrata*, the differences in neutral mutations between the diploid species and the corresponding subgenomes are far less remarkable in *A. kamchatica* than in *C. bursa-pastoris*. These data suggest that N_e alone is not adequate to explain the proportion of neutral mutations.

The strongest signal for relaxed constraint that we detected in the *A. kamchatica* subgenomes was observed when genes were categorized by expression levels. Genes that had low expression showed a significant increase in the proportion of neutral mutations (30-32%) over highly expressed genes (13-19%), and highly expressed genes show the strongest levels of purifying selection (for N_es > 10, 73-77% of mutations) in either subgenome. This result is consistent with expectations of stronger selective constraint on highly expressed genes[49]. A similar result was also found in the diploid *M. truncatula* where expression levels predicted very clearly the proportion of neutral mutations[51], adding further support that the method is able to detect large differences in relaxed constraint when gene expression levels are taken into account.

Although theoretical analysis typically assumes that deleterious mutations may be masked by genome duplication, empirical studies showed that the dosage balance in gene networks may be a selective constraint[52] and could work as a mechanism for purifying selection in an allopolyploid species. At this moment, the factors contributing to the difference between *A. kamchatica* and *C. bursa-pastoris* are not clear. It is possible that the time since the polyploidization events would not be adequate to detect the changes in the strength of purifying selection, although the time estimates of polyploidization overlap to a large extent (about 20,000-250,000 years ago for *A. kamchatica*, 100,000-300,000 years ago for *C. bursa-pastoris*).

The Proportion of Adaptive Substitutions (α) are Significantly Greater Than Zero

This is the first report of α for *A. halleri* and *A. lyrata* using whole genome data, and to our knowledge, the first report of genome-wide α for a polyploid species. Previous multi-species comparisons showed that only a few plant species have α values that are greater than zero[17], however these estimates were mostly done using limited genetic data (< 1000 loci)[17,19] rather than genome-wide data. We estimated that 25-27% of non-synonymous substitutions are adaptive in the two diploid species *A. halleri* and *A. lyrata*. These are the highest estimates of α

for any *Arabidopsis* species[17,40] and higher than most plant species. The highest α among any plant species was estimated in the highly outcrossing *Capsella grandiflora* (α = 0.4-0.7)[19,53] with levels similar to *Drosophila* and bacteria, all taxa with large effective population sizes[18]. Our results for the diploid species are consistent with previous studies that have shown a positive correlation between α and N_e[17,20] which suggests that greater adaptive evolution often occurs in species with large effective population sizes, which is true for both highly outcrossing diploid species reported here.

Importantly, α for both subgenomes of *A. kamchatica* is also significantly greater than zero and indicates 6-12% of non-synonymous substitutions are adaptive. Many diploid plant species have a similar or larger effective population size than *A. kamchatica* (54,000-77,000), but did not show positive α[17]. For example, N_e estimated for *A. thaliana* was between 65,000 – 267,000[17,20] while α = -0.08[19], indicating that effective population size alone cannot explain the significantly positive α of *A. kamchatica*. These data suggest that *A. kamchatica* has a positive α because of polyploidy. We suggest two mutually non-exclusive explanations. First, *A. kamchatica* may have inherited fixed non-synonymous or adaptive substitutions from the two parental species. The α values of *A. kamchatica* are roughly half of the parental species, in which the reduction may be attributable to the reduction of N_e. Second, the rate of non-synonymous mutations are increased at the early stages of polyploid species in contrast to slow rate of old duplicated genes[21,22]. A classic idea of the high evolvability of duplicated genomes states that one of the duplicated copies may be able to obtain a new function or adaptive mutations because the other copy retains the original function[23,24].

High Impact Mutations with Deleterious Effects Were Rarely Fixed

The loss of homeologs in ancient polyploids, or nonfunctionalization, has been extensively studied [24], but relatively little is known about the population genetics of young polyploid species. We identified high impact mutations that are likely to disrupt the gene function. We found that about 20% of the homeologs in both subgenomes had disruptive mutations in our collection of 25 individuals (Supplementary Table 7), although their frequencies are low (Fig. 5) and only rarely are both homeologs disrupted. Interestingly, we found that high impact mutations were rarely fixed. This is in contrast with the results from another allopolyploid species *C. bursa-pastoris*, in which a large proportion of high-impact mutations (such as stop codon gained) were fixed[8]. In *A. kamchatica*, similar proportions of high-impact mutations were

516 at low frequency compared with non-synonymous substitutions, which are also at low
517 frequency (Fig. 1B), suggesting that genome-wide purifying selection keeps their frequency low,
518 which is consistent with the prevalence of purifying selection shown by DoS and by DFE
519 methods.
520
521 ### Conclusion
522 Recently, new sequencing technology and algorithms drastically improved the genome assembly
523 of crop polyploid species with a large genome size[54–56] which will facilitate the genome-wide
524 polymorphism analysis and scans for selection. By quantifying selection using polyploid species
525 with different population sizes, times since polyploidization and mating systems, general
526 patterns of selection in polyploid genomes will emerge. A further step will be to incorporate
527 polymorphism, gene expression, and species distribution data (i.e., landscape genomics) of
528 diploid parents and allopolyploid hybrids to identify the contributions of parental adaptations
529 for broadening climatic regimes and abiotic habitats in polyploids.
530
531 ## Materials and Methods
532 ### Allopolyploid plant samples and resequencing
533 *Arabidopsis kamchatica* (Fisch. ex DC.) K. Shimizu & Kudoh[27] is an allotetraploid species
534 distributed in East Asia and North America. We consider Russian individuals described as
535 *Cardaminopsis kamtschatika* or *Cardaminopsis lyrata* as synonyms (note that *Arabidopsis lyrata*
536 is a distinct diploid species)[57]. Genomic DNA from 25 accessions of *A. kamchatica* was extracted
537 from leaf tissue using the D*Ne*asy Plant Kit (Qiagen). These accessions were collected from
538 Taiwan, lowland and highland regions of Japan, Eastern Russia, Sakhalin Island, and Alaska, USA
539 (listed in Supplementary Table 3). DNA concentration and quality was measured using Qbit.
540 Genomic DNA libraries were constructed at the Functional Genomics Center Zurich (FGCZ) using
541 NEB *Ne*xt Ultra. Total DNA was sequenced on Illumina HiSeq 2000 using paired end sequences
542 with an average insert size of 200-500 bp. Read lengths were 100 bp. For 22 accessions, a single
543 lane included six *A. kamchatica* DNA samples and for three accessions (KWS, MUR, and PAK),
544 eight samples per lane were used.
545
546 ### Illumina read mapping and sorting using v2.2 reference genomes

Illumina reads from *A. kamchatica* were mapped using BWA-MEM version 0.7.10 on the two diploid genomes independently. We classified the reads to each parental origin as H-origin (*halleri*-origin) and L-origin (*lyrata*-origin) using HomeoRoq (http://seselab.org/homeoroq, last accessed July 14, 2016). In this method, reads from each accession were first mapped to each parental genome, and then classified as H-origin, L-origin, common, or unclassified (see fig. 1 in[32] for schematic diagram). Here, the 'common' reads are the reads that aligned equally well to both parental genomes. After mapping to the *A. halleri* genome, we detected *A. kamchatica halleri*-origin (H-origin) reads and identified single-nucleotide polymorphisms (SNPs) and short insertions and deletions using GATK v3.3[58]. Then, the nucleotides were replaced on the detected variant position in the reference genome with the alternative nucleotides if the position (1) covered by at least 20% of the average coverage of reads in each library, (2) covered by at most twice of the average coverage and (3) has 30 or higher mutation detection quality (QUAL) produced by GATK. This cycle of mapping, read classification, and reference modification, was repeated ten times. For the reference modification, we used only *origin* reads the first five times and both origin and common reads the last five times. The *A. kamchatica lyrata*-origin (L-origin) genome was iteratively updated in a similar manner. The modified genomes were only used for read sorting. Coverage was calculated for both subgenomes of our resequenced lines by using the sum of the diploid parents as the genome size (250 + 225 = 475) and *common* plus sorted *origin* reads (Supplementary Table 3).

Variant calling

For final variant calling, we combined the common reads of *A. kamchatica* with each sorted H-origin or L-origin reads and aligned them back to the original parental genomes using BWA-MEM v0.7.10. We called variants using GATK v3.3-0 following established best practices[59,60]. We processed each alignment BAM file separately to fix mate pairs, mark duplicates, and realign reads around indels. Then we identified variants by running HaplotypeCaller jointly on all genotypes but separately for each parental subgenome. To remove low-quality variants, we mostly used the thresholds recommended for variant data sets where quality score cannot be recalibrated [60]. We applied quality by depth (QD < 2), mapping quality (MQ < 30), mapping quality rank sum (MQRankSum < -15) and genotype quality (GQ < 20) filters. Because some of our accessions had relatively low coverage, we considered that the recommended strand and read position filters might be too strict and we did not apply them. Finally, we removed all

579 variants that GATK reported as heterozygous. We used diploid data from 9 accessions of
580 European *A. halleri* and 9 accessions of European *A. lyrata* from Novikova et al.[30] mapped to our
581 diploid references genomes and called SNPs using the same criteria. The diploid VCF files were
582 then phased using Beagle[61] to produce 18 alleles for each species.
583 Regions with excessively high coverage are likely to be repetitive or incorrectly
584 assembled, therefore variants called in those regions are probably spurious. To determine the
585 coverage thresholds, we summed up the coverage reported by bamtools[62] for each position in
586 the final alignment files across all genotypes. We only considered reads with mapping quality
587 (MQ) of at least 20. Then, we calculated the mean and standard deviation for the distribution of
588 the obtained sums in each parental genome. We assumed a Poisson distribution and added 5
589 standard deviations to the mean to determine the thresholds. These thresholds (2891 and 2509
590 for *A. halleri* and *A. lyrata* respectively) were applied to the DP property (total depth of coverage
591 across all genotypes) in the INFO field of the corresponding VCF file. In addition, we applied a
592 coverage filter at genotype level to exclude calls with coverage below 2 or above 250.
593 To check for additional spurious variants, we randomly sampled 20 million reads (10
594 million per parent) from *A. halleri* and *A. lyrata* short-insert (200 bp) reads and ran it through
595 the same variant calling pipeline as the *A. kamchatica* genotypes. The only difference between
596 the runs was that this simulated sample was processed alone while variants for *A. kamchatica*
597 genotypes were called jointly. Any variants called with the simulated sample would be due to
598 incorrect read sorting between the parents or repetitive sequences present in the parental
599 genomes. Such spurious variants would also be likely to appear among *A. kamchatica* variants
600 even if the corresponding regions were completely conserved between *A. kamchatica* and its
601 parents. Among the uncovered variants, 59,856 and 58,645 were also present in *A. kamchatica*
602 on *A. halleri* and *A. lyrata* sides respectively. All of these variants were marked as filter failing.
603 When applying polymorphisms to the reference sequences, we used N's in positions where clear
604 calls could not be made due to insufficient coverage, excessive coverage, low quality
605 polymorphisms or heterozygosity. Such treatment allowed us to avoid using reference calls in
606 regions where the actual sequence is highly uncertain.
607
608 Coding sequence (CDS) alignments
609 We identified homeologous genes based on reciprocal blast hit (best-to-best with E-values < 10^{-15}
610 and alignment length ≥ 200 bp) among coding sequences from the v2.2 *A. halleri* and *A. lyrata*

genome annotations. Using the same approach, we also detected orthologous relationships between the predicted genes in diploid *A. halleri* and *A. lyrata* annotated genome assemblies and *A. thaliana* genes (TAIR 10). In cases of duplicated genes of interest such as *HMA4* (tandemly duplicated three times in *A. halleri*), we used only one copy for diversity analysis due to non-unique alignments of Illumina reads and very high sequence identity (99%) in the *A. halleri* reference genome. Therefore, our genome-wide dataset of coding sequences of homeologs do not contain genes that are duplicated in one genome but not the other.

To make coding sequence alignments, we individually applied SNPs and deletions from each of the 25 *A. kamchatica* genotypes (*H-origin* or *L-origin*) to the corresponding reference genomes. We omitted insertions in order to preserve the genomic coordinates of the coding sequences, which would consequently facilitate the alignment. If a variant was heterozygous, failed the genotype quality filter (GQ < 20), or was not called for a particular genotype (but called for other genotypes), the corresponding bases were replaced with N's. We assumed that a sequence contains reference bases at positions that are not specified in VCF file and have adequate coverage. Therefore, all bases with coverage < 2 (insufficient) or > 250 (abnormally high) were replaced with N's. After that, we extracted coding sequences from the modified genomes and grouped them by gene. Thus, each H-origin or L-origin gene had an alignment file containing 25 aligned coding sequences (one for each genotype). Finally, we aligned *A. thaliana* orthologs as an outgroup using Muscle v3.8[63]. With the profile alignment option, which preserved the alignment of the ingroup sequences and only aligned the outgroup sequence to the core ingroup alignment. The same procedure was used for making gene alignments of the 18 phased alleles for diploid *A. halleri* and *A. lyrata*.

Population structure and phylogenetic analysis

We used 1000 randomly selected coding sequence (CDS) alignments from both *halleri* and *lyrata* derived homeologs. We then individually concatenated the *halleri* alignments and the *lyrata* alignments to use for population structure and phylogenetic analysis. The input data sets for the population structure analysis contained 21,341 and 16,223 markers from *halleri*- and *lyrata*-origin CDS respectively. We ran STRUCTURE v2.3.4[64] ten times for each K = 1 to 9 using the admixture model and 50,000 MCMC rounds for burnin followed by 100,000 rounds to generate the data. The output was analyzed with STRUCTURE HARVESTER v0.6.94 and clusters were rearranged with CLUMPP v1.1.2. For phylogenetic analysis, we added *A. halleri* and *A. lyrata* as

643 outgroups and ran Mr. Bayes v3.2.6[65] with default parameters for 500,000 generations sampling
644 every 1000th generation.
645
646 ## Coding sequence diversity and site frequency spectra
647 For gene alignments containing coding sequences, summary and diversity statistics, including
648 divergence from *A. thaliana*, were estimated using *libsequence* packages [66] and custom R, Perl,
649 and Ruby shell scripts. The *libsequence* programs *compute* and *Hcalc* were used to estimates
650 average pairwise diversity (π), θ_w, Tajima's D, Fay and Wu's H. Non-synonymous and
651 synonymous diversity and gene based allele frequencies were estimated using the *polydNdS*
652 program with the –P flag to generate SNP tables for each gene. The site frequency spectra (SFS),
653 were created using the SFS.pl program available from the J. Ross-Ibarra
654 (http://www.plantsciences.ucdavis.edu/faculty/ross-
655 ibarra/code/files/ea3bd485e4c7dee37c59e8ba77ca800e-11.html) on the set of non-
656 synonymous and synonymous polymorphisms identified using *polydnds*. Both folded and
657 unfolded SFS were calculated; the folded spectrum does not differentiate between ancestral
658 polymorphisms and polymorphism that are the result of mutations that have entered a
659 population since it split from a common ancestor, while the unfolded spectra are based on
660 derived allele frequencies. We converted the SFS data to SFS count tables using a custom python
661 script (sfs_extraction.py). We used two published mutation rates, one based on the synonymous
662 substitution rates calibrated by fossil records[41], and another for total sites in mutation
663 accumulation lines[42], to estimate the effective population size using the following equation: N_e =
664 π_{syn} or π_{total} /4μ (where π was estimated from our data and μ from[41,42]).
665
666 ## Linkage disequilibrium and sliding window diversity
667 To conduct sliding window analyses along entire scaffolds, we used the PopGenome R[67] package
668 to calculate diversity of all, intergenic, coding, exonic, and intron regions of *A. kamchatica* using
669 *A. halleri* or *A. lyrata* derived VCF and reference gene annotation (.gff) files. We estimated the
670 average nucleotide diversity, Watterson's θ_w and π (the average number of pairwise nucleotide
671 differences per site). To estimate genome-wide linkage disequilibrium (LD), we used the geno-
672 r2 option in VCFtools[68] across window sizes of a maximum distance of 20 kb, 50 kb or 1 Mb using
673 a minor allele frequency ≥ 0.1, separately for the halleri or lyrata derived VCF files. The resulting

674 r^2 between SNPs were grouped into bins of 50 bp length. We estimated the average, 50% and
675 90% confidence intervals of correlation coefficients of each bin.
676
677 ## Direction of selection (DoS), Distribution of Fitness Effects (DFE) and Adaptive
678 ## Substitutions (α)
679 The program *MKtest* from the libsequence library, was used to count the total number of
680 polymorphic non-synonymous (P_n) and synonymous (P_s) sites in *A. kamchatica* homeologs as
681 well as the number of fixed non-synonymous (D_n) and synonymous (D_s) differences between *A.*
682 *kamchatica* homeologs and *A. thaliana*. We used the program *MKtest* to perform standard tests
683 on each gene for both homeologs separately; this is a contingency test comparing the numbers
684 of between species difference and within species polymorphisms at non-synonymous and
685 synonymous sites where significance is tested using Fisher's exact tests for each gene.
686 Polymorphism and divergence data was used to calculate the direction of selection (DoS
687 = $D_n/(D_n+ D_s) - P_n/(P_n + P_s)$) statistic of [14]. DoS < 0 is consistent with purifying selection and DoS >
688 0 is consistent with positive selection. To estimate the distribution of fitness effects (DFE, i.e. the
689 distribution of the strength of selection acting against new mutations) and the proportion of
690 adaptive substitutions (α) in *A. kamchatica*, *A. halleri* and *A. lyrata*, we used the likelihood
691 method implemented in the software DoFE 3.0[13]. The program was run for $1x10^6$ steps, and
692 sampled every 1,000 steps after a burn in of 100,000 steps. Strongly deleterious mutations have
693 $N_es > 10$ (where N_e is the effective population size and s is the selection coefficient), mildly
694 deleterious mutations have $1 < N_es < 10$, and effectively neutral mutations have $N_es < 1$. To
695 estimate DFE we used folded allele frequency spectra and the estimated number of non-
696 synonymous (D_n) and synonymous (D_s) differences between *A. kamchatica* homeologs or diploid
697 orthologs and the corresonding outgroup *A. thaliana* orthologs.
698
699 ## Transcriptome data
700 We used RNA-seq data collected from roots and leaf tissue of the *A. kamchatica* Murodo (Japan)
701 and Potter (Alaska, USA) accessions from Paape et al. 2016 to calculate expression for all
702 homeologs in our dataset. We mapped the RNA-seq data to v2.2 *A. halleri* and *A. lyrata*
703 reference genomes and sorted the reads using method described in Akama et al. 2014. Thus, for
704 each gene in our polymorphism dataset, we obtained expression data that is specific to either
705 homeolog. We estimated expression levels using HTseq to count reads, then calculated reads

706 per kilobase of transcript per million mapped reads (RPKM). The mean RPKM values from three
707 libraries of both leaf and root were used to make a distribution in RPKM that corresponds to our
708 polymorphism gene dataset. The distribution of RPKM was used to determine the upper and
709 lower 10% tails in expression for both homeologs separately.
710
711 ## Detection of High Impact Mutations
712 We used SnpEff v4.2[69] to detect genetic variants that have putative loss of function mutations in
713 both subgenomes of *A. kamchatica*. We ran the program separately on the variant file of each
714 subgenome. First, we built custom databases for each parental genome using our v2.2 parental
715 assemblies and annotation. Since SnpEff ignores filter fields in VCF files, we have removed all
716 variants that failed our filters, replaced all genotypes that failed genotype filters with no-calls
717 (i.e. './.'), and removed any entries without valid variant calls. Such filtering allowed us to extract
718 accurate gene summaries from SnpEff output.
719 SnpEff annotated polymorphisms within 32,410 and 31,119 genic regions in *A. halleri*
720 derived and *A. lyrata* derived genomes respectively. These include all mutations with any impact
721 type, but we focused only on frameshifts, premature stop codon, loss of stop codons and loss of
722 start codons. The gene sets were thus reduced to 31,193 and 31,119 genes for *A. halleri* and *A.*
723 *lyrata* derived genomes respectively. There are 21,419 and 21,463 reciprocal best BLAST hits
724 between respectively *A. halleri* or *A. lyrata* and *A. thaliana*. Based on the intersection of these
725 two data sets, we identified 20,292 homeologs between *A. halleri* and *A. lyrata*. Out of these 19
726 and 18 *halleri*-origin and *lyrata*-origin genes had no coverage. Gene ontology (GO) analysis was
727 perfomed using agriGO (bioinfo.cau.edu.cn/agriGO) conducted using a custom annotation
728 containing 19,936 GO annotations that correspond to *A. thaliana* orthologs with reciprocal-best
729 BLAST hits for both homeologs. We used only queries with at least 20 genes.
730
731
732 ## Acknowledgments
733 We thank Takashi Tsuchimatsu, Polina Novikova and Peter Keightley for useful discussions, and
734 the Functional Genomic Center Zurich for sequencing services and technical support. The study
735 was supported by Swiss National Science Foundation, the University Research Priority Program
736 of Evolution in Action of the University of Zurich, JST CREST Grant (number JPMJCR16O3) to KKS,
737 MEXT KAKENHI Grant Number 16H06469, 26113709, Young Investigator Award of Human

Frontier Science Program to KKS and JS, European Union's Seventh Framework Programme for research, technological development and demonstration under grant agreement no GA-2010-267243 – PLANT FELLOWS to RVB and TP, Marie-Heim Hoegtlin grant by Swiss National Science Foundation to RSI, ISCB (Indo-Swiss Collaboration in Biotechnology) to KKS and MH, the Special Coordination Funds for Promoting Science and Technology from MEXT Japan, an Inamori Foundation research grant, a Japan Society for the Promotion of Science Grant-in-Aid for Scientific Research (Young Researchers B, 2277023), and Research and Education Funding for Japanese Alps Inter-Universities Cooperative Project, MEXT, Japan to KT.

Data Accessibility

Illumina reads submitted to DDBJ. BioProject Submission ID: PSUB006170
The Sanger sequences were submitted to GenBank. GenBank BankIt submission. Submission ID: 2025864

Code for A. lyrata genome assembly
https://gitlab.com/rbrisk/AlyrAssembly

Code for Variant calling in *A. kamchatica*
https://gitlab.com/rbrisk/AkamVariants

Figures.

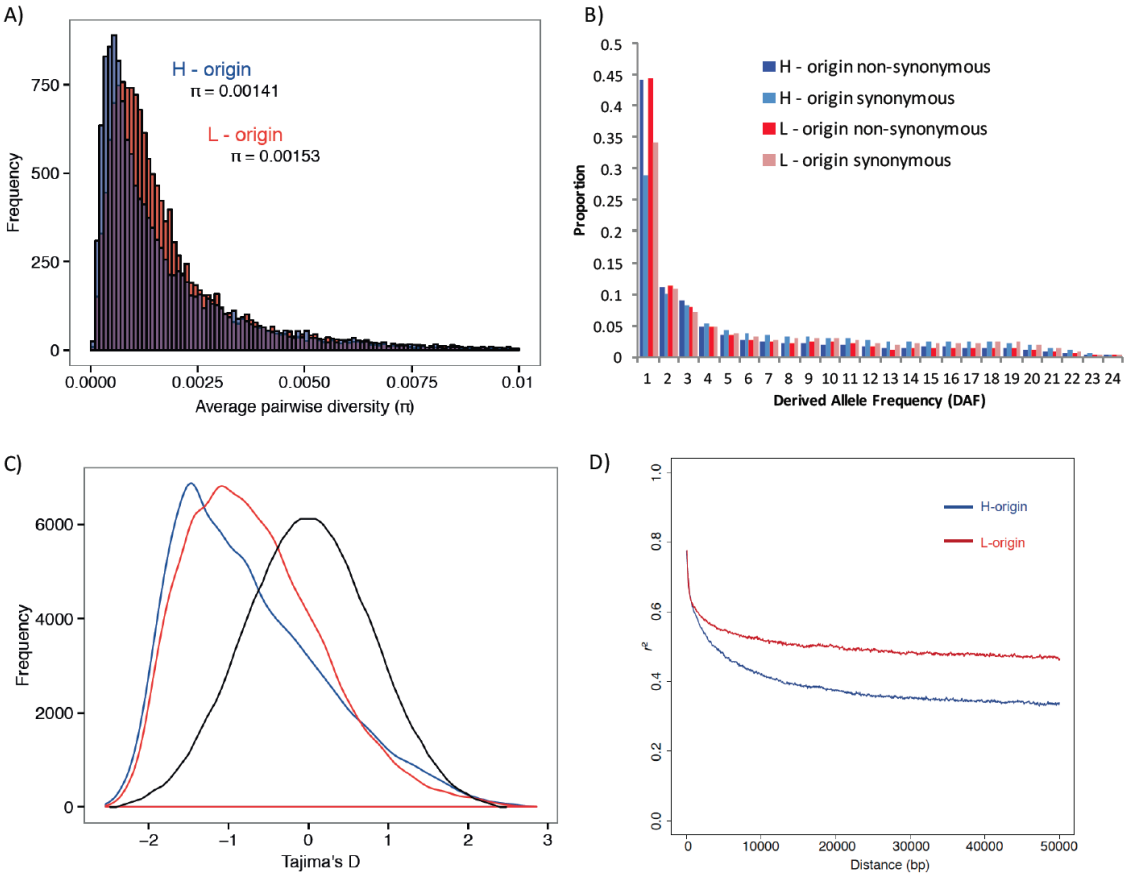

Fig. 1. Genome-wide diversity and linkage disequilibrium. (A) Average pairwise diversity (π) of *halleri*-origin (H-origin) and *lyrata*-origin (L-origin) coding sequences. (B) H-origin and L-origin genes show no significant differences in proportions of non-synonymous and synonymous substitutions (X^2, p-value = 0.58), and the majority of substitutions are low at frequency. (C) Tajima's D distributions for both genomes (blue density curve = H-origin, red density curve = L-origin) show departures from neutrality (black density curve where neutral = 0), mean values for both distributions are negative (Table 1). (D) The mean decay of linkage disequilibrium (LD) estimated using 100 kb sliding windows shows mean LD decay < 10 kb for both H-origin (blue) and L-origin (red) genomes.

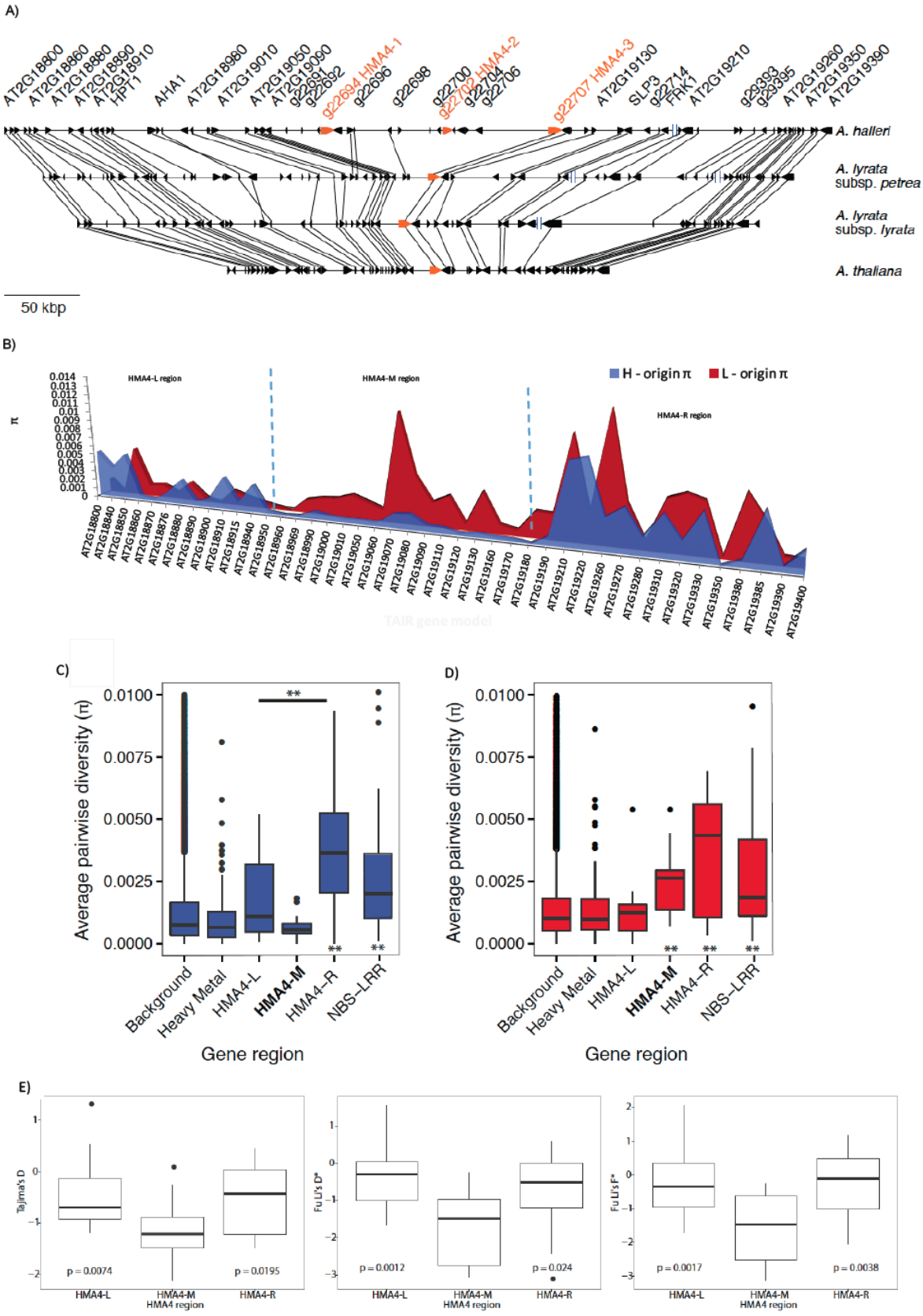

786

Fig. 2. **Genetic diversity of the syntenic *HMA4* region.** (A) Synteny of the *HMA4* region from *A. halleri* v2.2[39], *A. lyrata* subsp. *petraea* v2.2, *A. lyrata* subsp. *lyrata* (JGI)[70] and *A. thaliana* (TAIR). (B) Average pairwise diversity (π) of genes surrounding the *HMA4* region in both homeologs of *A. kamchatica*. (C) For the *halleri*-subgenome, genetic diversity of NBS-LRRs is significantly greater (two asterisks below, **p < 0.001) than diversity compared with the background while heavy metal (HM) genes show no significant difference. Diversity for both HMA4-L (π = 0.0018) and HMA4-R (π = 0.004) are significantly higher than the HMA4-M (which contains the *HMA4* coding sequences) region (two asterisks above HMA4-M, **p < 0.001). (D) For the *lyrata*-subgenome, diversity of NBS-LRRs, HMA4-M and HMA4-R are all significantly higher than the background. The diversity of the *lyrata* HMA4-M (π = 0.0032) region is also significantly greater than the *halleri* HMA4-M region (π = 0.0007, paired *t-test* p-value = 0.003; Wilcoxon sign rank p-value = 0.0001). The neutrality statistics (E) Tajima's D, Fu and Li's D* and Fu and Li's F* all show the *halleri*-origin HMA4-M region to be significantly lower than the left and right flanking regions supporting genetic hitchhiking surrounding the *HMA4* coding sequences.

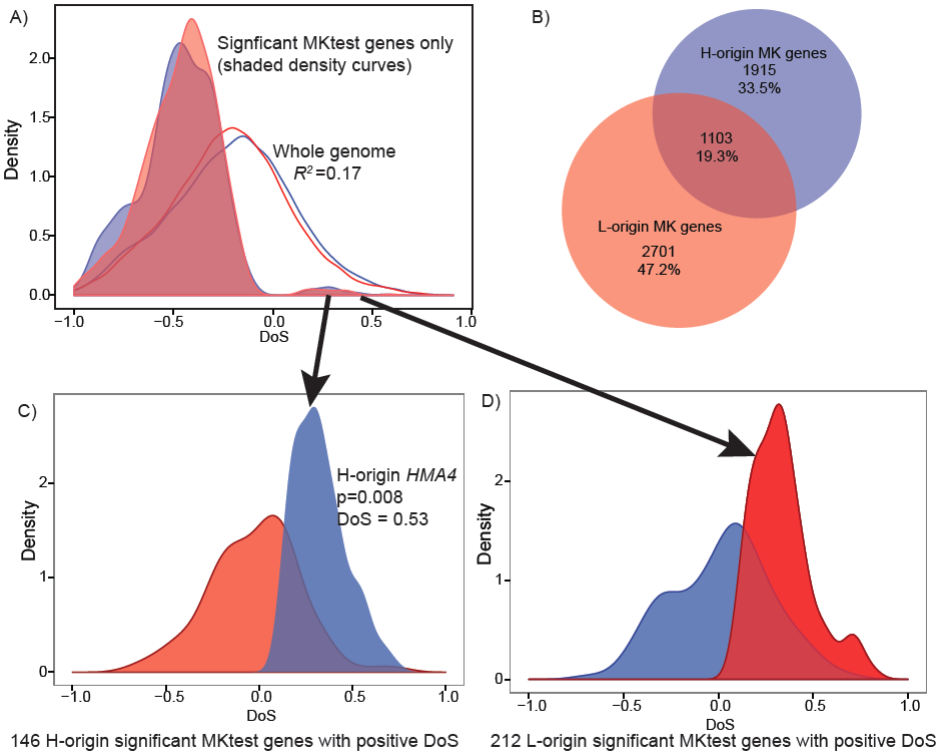

Fig. 3. **The direction of selection for both subgenomes**. (A) Density curves of the direction of selection (DoS)[14] for about 21,000 coding sequences (blue line and density curves are DoS for H-origin genes, red line and density are DoS for L-origin genes). *Ne*utral genes are indicated by 0, while negative values indicate purifying selection and positive values indicate positive selection. The means of these distributions are -0.20 and -0.22 for the H- and L-origin homeologs respectively, and show that ~70% of both homeologs have a negative selection index (negative DoS). Shaded density curves are genes that were significant for MK-tests ($p < 0.05$ using Fisher's marginal p-values). (B) Only 19% of genes show significance for MK-tests for both homeologs. (C) Using only significant MK-test genes with positive DoS for *halleri*-origin and (D) positive DoS for *lyrata*-origin genes show that the other homeolog has significantly more negative DoS (p-value < 2.2e-16 using pairwise t-test and Wilcoxon signed rank test) when one shows positive selection using comparisons of DoS distributions in both C and D.

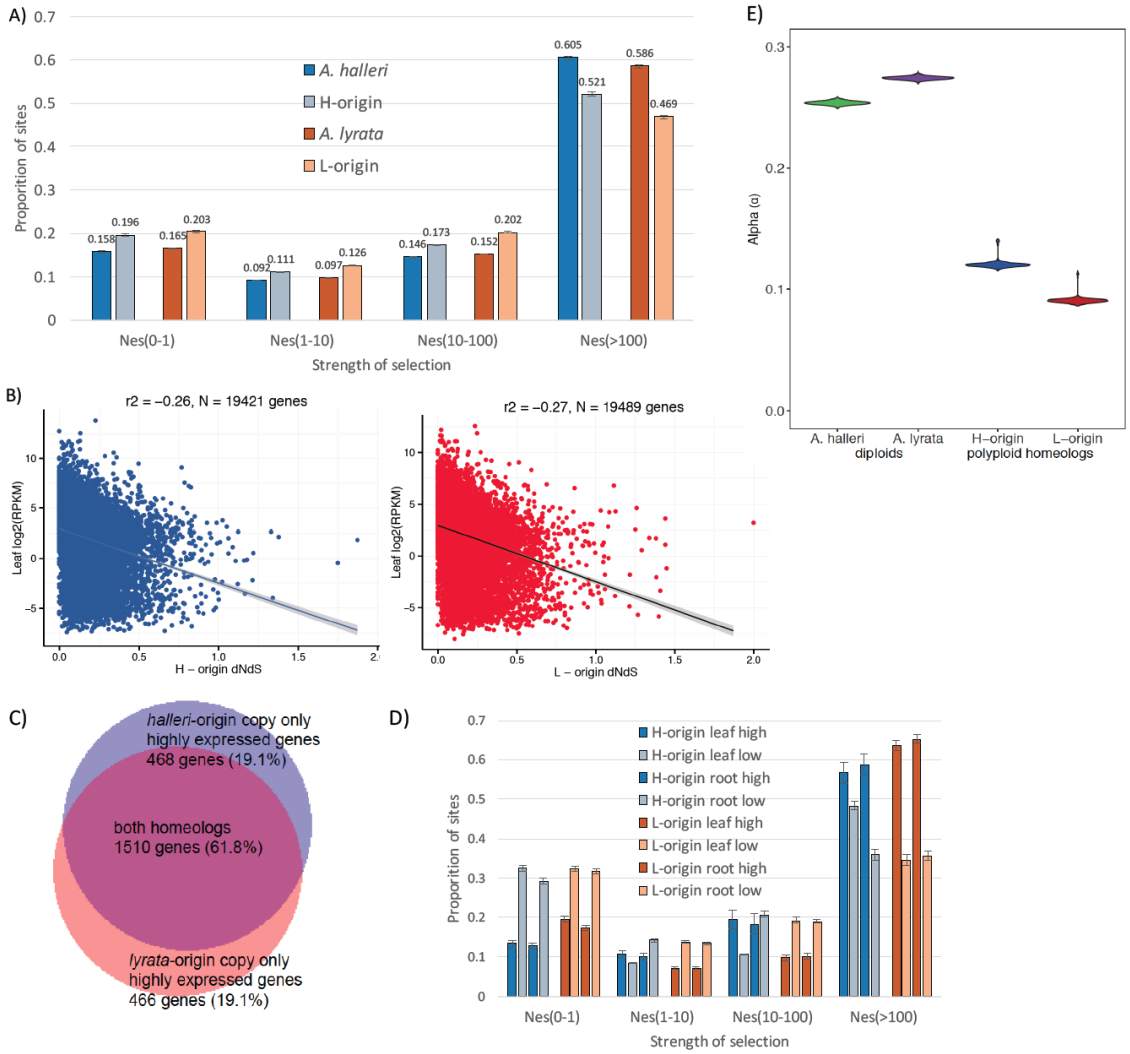

Fig. 4. The strength of purifying selection and adaptive evolution. (A) The distribution of fitness effects (DFE) of deleterious mutations for coding sequences of the two *A. kamchatica* subgenomes and corresponding diploid orthologs of *A. halleri* and *A. lyrata*. The strength of selection is indicated by $N_e s$ where N_e is the effective population size and s is the selection coefficient. Error bars show standard deviations. (B) Evolutionary rates are negatively correlated with gene expression in both homeologs. (C) Overlap of genes that are highly expressed leaf tissues (in upper 10% of expression) in both homeologs. (D) DFE categorized by expression in both subgenomes. Expression categories were taken from the upper 10% (high) and lower 10% (low) of expression distribution in all *A. kamchatica* homeologs. (E) The proportion of adaptive substitutions (α) for both subgenomes (H-origin α = 0.12, CI: 0.117- 0.141, L-origin α = 0.09, CI: 0.087-0.094) and for the two corresponding diploid species (*A. halleri* α = 0.25, CI: 0.251-0.257, *A. lyrata* α = 0.27, CI: 0.272-0.277) are significantly greater than zero.

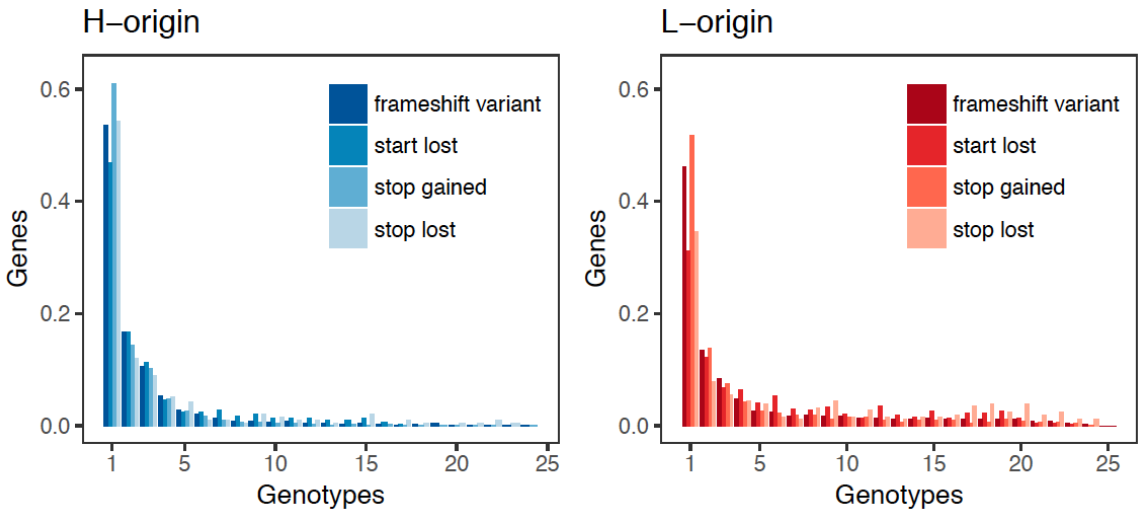

Fig. 5. **Frequency distributions of high impact mutations.** Large effect mutations are at low frequency for both subgenomes.

877 **Tables**

878

879 Table 1. Reference genome assembly statistics of v2.2 of Siberian *A. lyrata* subsp. *petraea* and

880 v2.2 of *A. halleri* subsp. *gemmifera* (Tada Mine).

881

Assembly statistics	*A. lyrata*	*A. halleri*[a]
Length (bp)	175,182,717	196,243,198
Missing (%)[b]	12.75	14.81
Scaffolds	1,675	2,239
Shortest scaffolds (bp)	940	932
Longest scaffolds (bp)	6,771,235	4,302,264
Scaffold N50 length (bp)	1,260,070	712,249
Scaffold N50 count	38	71
NG50 length (bp)	804,357	489,153
NG50 count	63	117
Genome size (FC)[c]	225 Mb	250 Mb

a: *A. halleri* assembly previously reported in Briskine et al.[39]

b: Missing data counted as number of N's in the assembly and is percentage of total length

c: Genome size measured by flow cytometry (FC)

882

883

884

885

886

887

888

889

890

891

892

893

894

895

896

897

Table 2. Diversity statistics for coding sequences (CDS) of *A. kamchatica* homeologs. Values are average pairwise diversity, π, polymorphism Watterson's estimator, θ_w, Tajima's D, Fay and Wu's H. Correlations between homeolog diversity stastistics are shown as R^2 correlation coefficient.

	***halleri* homeologs**			***lyrata* homeologs**				**combined**		
statistic	**mean**	**sd**	**n**	**mean**	**sd**	**n**	R^2	mean	sd	n
π_{total}	0.0014	0.0019	21419	0.0015	0.0018	21463	0.27	0.0015	0.0015	20249
θ_w	0.0017	0.0018	21419	0.0018	0.0019	21463	0.30	0.0017	0.0015	20249
π_{nonsyn}	0.0011	0.0029	20605	0.0014	0.0033	20696	0.15	0.0012	0.0025	19953
π_{syn}	0.0044	0.0116	20605	0.0049	0.0343	20696	0.04	0.0046	0.0182	20249
$\theta_{w\ nonsyn}$	0.0014	0.0029	20605	0.0017	0.0034	20696	0.14	0.0012	0.0025	19953
$\theta_{w\ syn}$	0.0047	0.0114	20605	0.0056	0.0344	20696	0.04	0.0051	0.0183	19953
Taj D	-0.72	0.89	19691	-0.63	0.85	19984	0.03	-0.67	0.66	19940
FayWuH	-0.41	1.23	19574	-0.49	1.28	19893	0.07	-0.44	0.97	19911

nonsynon = non-synonymous substitutions

synon = synonymous substitutions

927 **References**

928 1. Wood, T. E. *et al.* The frequency of polyploid speciation in vascular plants. *Proc. Natl. Acad. Sci.* **106,**
929 13875–13879 (2009).
930 2. Renny-Byfield, S. & Wendel, J. F. Doubling down on genomes: Polyploidy and crop plants. *Am. J. Bot.*
931 **101,** 1711–1725 (2014).
932 3. Comai, L. The advantages and disadvantages of being polyploid. *Nat. Rev. Genet.* **6,** 836–846 (2005).
933 4. Soltis, D. E., Visger, C. J. & Soltis, P. S. The polyploidy revolution then...and now: Stebbins revisited.
934 *Am. J. Bot.* **101,** 1057–1078 (2014).
935 5. Dufresne, F., Stift, M., Vergilino, R. & Mable, B. K. Recent progress and challenges in population
936 genetics of polyploid organisms: an overview of current state-of-the-art molecular and statistical
937 tools. *Mol. Ecol.* **23,** 40–69 (2014).
938 6. Buggs, R. J. A. *et al.* Next-generation sequencing and genome evolution in allopolyploids. *Am. J. Bot.*
939 **99,** 372–382 (2012).
940 7. Clevenger, J., Chavarro, C., Pearl, S. A., Ozias-Akins, P. & Jackson, S. A. Single Nucleotide
941 Polymorphism Identification in Polyploids: A Review, Example, and Recommendations. *Mol. Plant* **8,**
942 831–846 (2015).
943 8. Douglas, G. M. *et al.* Hybrid origins and the earliest stages of diploidization in the highly successful
944 recent polyploid *Capsella bursa-pastoris*. *Proc. Natl. Acad. Sci.* **112,** 2806–2811 (2015).
945 9. Arnold, B. J. *et al.* Borrowed alleles and convergence in serpentine adaptation. *Proc. Natl. Acad. Sci.*
946 **113,** 8320–8325 (2016).
947 10. Paape, T. *et al.* Conserved but Attenuated Parental Gene Expression in Allopolyploids: Constitutive
948 Zinc Hyperaccumulation in the Allotetraploid *Arabidopsis kamchatica*. *Mol. Biol. Evol.* **33,** 2781–
949 2800 (2016).
950 11. Novikova, P. *et al.* Genome sequencing reveals the origin of the allotetraploid *Arabidopsis suecica*.
951 *Mol. Biol. Evol.* msw299 (2017). doi:10.1093/molbev/msw299
952 12. Nielsen, R. MOLECULAR SIGNATURES OF NATURAL SELECTION. *Annu. Rev. Genet.* **39,** 197–218
953 (2005).

13. Eyre-Walker, A. & Keightley, P. D. Estimating the Rate of Adaptive Molecular Evolution in the Presence of Slightly Deleterious Mutations and Population Size Change. *Mol. Biol. Evol.* **26,** 2097–2108 (2009).

14. Stoletzki, N. & Eyre-Walker, A. Estimation of the Neutrality Index. *Mol. Biol. Evol.* **28,** 63–70 (2010).

15. Hough, J., Williamson, R. J. & Wright, S. I. Patterns of Selection in Plant Genomes. *Annu. Rev. Ecol. Evol. Syst.* **44,** 31–49 (2013).

16. Otto, S. P. & Whitton, J. Polyploid Incidence and Evolution. *Annu. Rev. Genet.* **34,** 401–437 (2000).

17. Gossmann, T. I. *et al.* Genome Wide Analyses Reveal Little Evidence for Adaptive Evolution in Many Plant Species. *Mol. Biol. Evol.* **27,** 1822–1832 (2010).

18. Siol, M., Wright, S. I. & Barrett, S. C. H. The population genomics of plant adaptation. *New Phytol.* **188,** 313–332 (2010).

19. Slotte, T., Foxe, J. P., Hazzouri, K. M. & Wright, S. I. Genome-Wide Evidence for Efficient Positive and Purifying Selection in Capsella grandiflora, a Plant Species with a Large Effective Population Size. *Mol. Biol. Evol.* **27,** 1813–1821 (2010).

20. Gossmann, T. I., Keightley, P. D. & Eyre-Walker, A. The Effect of Variation in the Effective Population Size on the Rate of Adaptive Molecular Evolution in Eukaryotes. *Genome Biol. Evol.* **4,** 658–667 (2012).

21. Jordan, I. K., Wolf, Y. I. & Koonin, E. V. Duplicated genes evolve slower than singletons despite the initial rate increase. *BMC Evol. Biol.* **4,** 22 (2004).

22. Yang, L. & Gaut, B. S. Factors that Contribute to Variation in Evolutionary Rate among Arabidopsis Genes. *Mol. Biol. Evol.* **28,** 2359–2369 (2011).

23. Ohno, S. *Evolution by Gene Duplication*. (Springer Berlin, 2014).

24. Lynch, M. & Conery, J. The Evolutionary Fate and Consequences of Duplicate Genes. *Science* **290,** 1151–1155 (2000).

25. Shimizu, K. K. & Tsuchimatsu, T. Evolution of Selfing: Recurrent Patterns in Molecular Adaptation. *Annu. Rev. Ecol. Evol. Syst.* **46,** 593–622 (2015).

26. Bomblies, K. & Madlung, A. Polyploidy in the Arabidopsis genus. *Chromosome Res.* **22,** 117–134 (2014).

27. Shimizu, Kentaro K, Fuji, S, Marhold, Karol, Watanabe, Kunaiki & Kudoh, Hiroshi. Arabidopsis kamchatica (Fisch. ex DC.) K. Shimizu & Kudoh and A. kamchatica subsp. kawasakiana (Makino) K. Shimizu & Kudoh, New Combinations. *Acta Phytotaxon. Geobot.* **56,** (2005).

28. Tsuchimatsu, T., Kaiser, P., Yew, C.-L., Bachelier, J. B. & Shimizu, K. K. Recent Loss of Self-Incompatibility by Degradation of the Male Component in Allotetraploid Arabidopsis kamchatica. *PLoS Genet.* **8,** e1002838 (2012).

29. Shimizu-Inatsugi, R. *et al.* The allopolyploid *Arabidopsis kamchatica* originated from multiple individuals of *Arabidopsis lyrata* and *Arabidopsis halleri*. *Mol. Ecol.* **18,** 4024–4048 (2009).

30. Novikova, P. Y. *et al.* Sequencing of the genus Arabidopsis identifies a complex history of nonbifurcating speciation and abundant trans-specific polymorphism. *Nat. Genet.* (2016). doi:10.1038/ng.3617

31. Schmickl, R., Jørgensen, M. H., Brysting, A. K. & Koch, M. A. The evolutionary history of the Arabidopsis lyrata complex: a hybrid in the amphi-Beringian area closes a large distribution gap and builds up a genetic barrier. *BMC Evol. Biol.* **10,** 98 (2010).

32. Akama, S., Shimizu-Inatsugi, R., Shimizu, K. K. & Sese, J. Genome-wide quantification of homeolog expression ratio revealed nonstochastic gene regulation in synthetic allopolyploid Arabidopsis. *Nucleic Acids Res.* **42,** e46–e46 (2014).

33. Armstrong, J. J., Takebayashi, N., Sformo, T. & Wolf, D. E. Cold tolerance in Arabidopsis kamchatica. *Am. J. Bot.* **102,** 439–448 (2015).

34. Hoffmann, M. H. EVOLUTION OF THE REALIZED CLIMATIC NICHE IN THE GENUS: ARABIDOPSIS (BRASSICACEAE). *Evolution* **59,** 1425–1436. (2005).

35. Kenta, T. Clinal Variation in Flowering Time and Vernalisation Requirement across a 3000-M Altitudinal Range in Perennial Arabidopsis kamchatica Ssp.Kamchatica and Annual Lowland Subspecies Kawasakiana. *J. Ecosyst. Ecography* **03,** (2013).

1006 36. Roux, C. *et al.* Does Speciation between Arabidopsis halleri and Arabidopsis lyrata Coincide with
1007 Major Changes in a Molecular Target of Adaptation? *PLoS ONE* **6,** e26872 (2011).
1008 37. Hanikenne, M. *et al.* Evolution of metal hyperaccumulation required cis-regulatory changes and
1009 triplication of HMA4. *Nature* **453,** 391–395 (2008).
1010 38. Hanikenne, M. *et al.* Hard Selective Sweep and Ectopic Gene Conversion in a Gene Cluster Affording
1011 Environmental Adaptation. *PLoS Genet.* **9,** e1003707 (2013).
1012 39. Briskine, R. V. *et al.* Genome assembly and annotation of *Arabidopsis halleri* , a model for heavy
1013 metal hyperaccumulation and evolutionary ecology. *Mol. Ecol. Resour.* (2016). doi:10.1111/1755-
1014 0998.12604
1015 40. Slotte, T. *et al.* Genomic Determinants of Protein Evolution and Polymorphism in Arabidopsis.
1016 *Genome Biol. Evol.* **3,** 1210–1219 (2011).
1017 41. Koch, M. A., Haubold, B. & Mitchell-Olds, T. Comparative Evolutionary Analysis of Chalcone
1018 Synthase and Alcohol Dehydrogenase Loci in Arabidopsis, Arabis, and Related Genera
1019 (Brassicaceae). *Mol. Biol. Evol.* **17,** 1483–1498 (2000).
1020 42. Ossowski, S. *et al.* The Rate and Molecular Spectrum of Spontaneous Mutations in Arabidopsis
1021 thaliana. *Science* **327,** 92–94 (2010).
1022 43. Nordborg, M. *et al.* The Pattern of Polymorphism in Arabidopsis thaliana. *PLoS Biol.* **3,** e196 (2005).
1023 44. Branca, A. *et al.* PNAS Plus: Whole-genome nucleotide diversity, recombination, and linkage
1024 disequilibrium in the model legume Medicago truncatula. *Proc. Natl. Acad. Sci.* (2011).
1025 doi:10.1073/pnas.1104032108
1026 45. Cao, J. *et al.* Whole-genome sequencing of multiple Arabidopsis thaliana populations. *Nat. Genet.*
1027 **43,** 956–963 (2011).
1028 46. Verbruggen, N., Hermans, C. & Schat, H. Molecular mechanisms of metal hyperaccumulation in
1029 plants: Tansley review. *New Phytol.* **181,** 759–776 (2009).
1030 47. Guo, Y.-L. *et al.* Genome-Wide Comparison of Nucleotide-Binding Site-Leucine-Rich Repeat-
1031 Encoding Genes in Arabidopsis. *PLANT Physiol.* **157,** 757–769 (2011).

48. Marone, D., Russo, M., Laidò, G., De Leonardis, A. & Mastrangelo, A. Plant Nucleotide Binding Site–Leucine-Rich Repeat (NBS-LRR) Genes: Active Guardians in Host Defense Responses. *Int. J. Mol. Sci.* **14,** 7302–7326 (2013).

49. Zhang, J. & Yang, J.-R. Determinants of the rate of protein sequence evolution. *Nat. Rev. Genet.* **16,** 409–420 (2015).

50. Yew, C.-L., Kakui, H. & Shimizu, K. K. Agrobacterium-mediated floral dip transformation of the model polyploid species Arabidopsis kamchatica. *J. Plant Res.* (2017). doi:10.1007/s10265-017-0982-9

51. Paape, T. *et al.* Selection, genome-wide fitness effects and evolutionary rates in the model legume *Medicago truncatula*. *Mol. Ecol.* **22,** 3525–3538 (2013).

52. Bekaert, M., Edger, P. P., Pires, J. C. & Conant, G. C. Two-Phase Resolution of Polyploidy in the *Arabidopsis* Metabolic Network Gives Rise to Relative and Absolute Dosage Constraints. *Plant Cell* **23,** 1719–1728 (2011).

53. Williamson, R. J. *et al.* Evidence for Widespread Positive and Negative Selection in Coding and Conserved Noncoding Regions of Capsella grandiflora. *PLoS Genet.* **10,** e1004622 (2014).

54. Hatakeyama, M. *et al.* Multiple hybrid de novo genome assembly of finger millet, an orphan allotetraploid crop. *DNA Res.* (2017). doi:10.1093/dnares/dsx036

55. Yang, J. *et al.* The genome sequence of allopolyploid Brassica juncea and analysis of differential homoeolog gene expression influencing selection. *Nat. Genet.* **48,** 1225–1232 (2016).

56. Avni, R. *et al.* Wild emmer genome architecture and diversity elucidate wheat evolution and domestication. *Science* **357,** 93–97 (2017).

57. S. Charkevics. *Plantae Vasculares Orientis Extremi Sovietici vol. 3, p. 101, 1988).* **3,** (1988).

58. McKenna, A. *et al.* The Genome Analysis Toolkit: A MapReduce framework for analyzing next-generation DNA sequencing data. *Genome Res.* **20,** 1297–1303 (2010).

59. DePristo, M. A. *et al.* A framework for variation discovery and genotyping using next-generation DNA sequencing data. *Nat. Genet.* **43,** 491–498 (2011).

60. Van der Auwera, G. A. *et al.* From FastQ data to high-confidence variant calls: The Genome Analysis Toolkit best practices pipeline. *Curr. Protoc. Bioinforma.* **43,** 11.10.1-11.10.33 (2013).

1059 61. Browning, S. R. & Browning, B. L. Rapid and Accurate Haplotype Phasing and Missing-Data Inference
1060 for Whole-Genome Association Studies By Use of Localized Haplotype Clustering. *Am. J. Hum.*
1061 *Genet.* **81,** 1084–1097 (2007).
1062 62. Barnett, D. W., Garrison, E. K., Quinlan, A. R., Strömberg, M. P. & Marth, G. T. BamTools: a C++ API
1063 and toolkit for analyzing and managing BAM files. *Bioinformatics* **27,** 1691–1692 (2011).
1064 63. Edgar, R. C. MUSCLE: multiple sequence alignment with high accuracy and high throughput. *Nucleic*
1065 *Acids Res.* **32,** 1792–1797 (2004).
1066 64. Pritchard, J. K., Stephens, M. & Donnelly, P. Inference of population structure using multilocus
1067 genotype data. *Genetics* **155,** 945–959 (2000).
1068 65. Ronquist, F. *et al.* MrBayes 3.2: Efficient Bayesian Phylogenetic Inference and Model Choice Across a
1069 Large Model Space. *Syst. Biol.* **61,** 539–542 (2012).
1070 66. Thornton, K. libsequence: a C++ class library for evolutionary genetic analysis. *Bioinformatics* **19,**
1071 2325–2327 (2003).
1072 67. Pfeifer, B., Wittelsburger, U., Ramos-Onsins, S. E. & Lercher, M. J. PopGenome: An Efficient Swiss
1073 Army Knife for Population Genomic Analyses in R. *Mol. Biol. Evol.* **31,** 1929–1936 (2014).
1074 68. Danecek, P. *et al.* The variant call format and VCFtools. *Bioinformatics* **27,** 2156–2158 (2011).
1075 69. Cingolani, P. *et al.* A program for annotating and predicting the effects of single nucleotide
1076 polymorphisms, SnpEff: SNPs in the genome of Drosophila melanogaster strain w ^{1118} ; iso-2; iso-3.
1077 *Fly (Austin)* **6,** 80–92 (2012).
1078 70. Hu, T. T. *et al.* The Arabidopsis lyrata genome sequence and the basis of rapid genome size change.
1079 *Nat. Genet.* **43,** 476–481 (2011).
1080
1081